

2007

## Design and Performance of a Curved-crystal X-ray Emission Spectrometer

A. C. Hudson  
*University of Nevada, Las Vegas*

Wayne C. Stolte  
*University of Nevada, Las Vegas, wcstolte@lbl.gov*

Dennis W. Lindle  
*University of Nevada, Las Vegas, lindle@unlv.nevada.edu*

Renaud Guillemin  
*CNRS, Laboratoire de Chimie Physique-Matière et Rayonnement*

Follow this and additional works at: [https://digitalscholarship.unlv.edu/chem\\_fac\\_articles](https://digitalscholarship.unlv.edu/chem_fac_articles)

 Part of the [Atomic, Molecular and Optical Physics Commons](#), [Biological and Chemical Physics Commons](#), and the [Physical Chemistry Commons](#)

### Repository Citation

Hudson, A. C., Stolte, W. C., Lindle, D. W., Guillemin, R. (2007). Design and Performance of a Curved-crystal X-ray Emission Spectrometer. *Review of Scientific Instruments*, 78(053101), 6.  
[https://digitalscholarship.unlv.edu/chem\\_fac\\_articles/18](https://digitalscholarship.unlv.edu/chem_fac_articles/18)

This Article is protected by copyright and/or related rights. It has been brought to you by Digital Scholarship@UNLV with permission from the rights-holder(s). You are free to use this Article in any way that is permitted by the copyright and related rights legislation that applies to your use. For other uses you need to obtain permission from the rights-holder(s) directly, unless additional rights are indicated by a Creative Commons license in the record and/or on the work itself.

This Article has been accepted for inclusion in Chemistry and Biochemistry Faculty Publications by an authorized administrator of Digital Scholarship@UNLV. For more information, please contact [digitalscholarship@unlv.edu](mailto:digitalscholarship@unlv.edu).

## Design and performance of a curved-crystal x-ray emission spectrometer

A. C. Hudson, W. C. Stolte, D. W. Lindle, and R. Guillemin

Citation: *Rev. Sci. Instrum.* **78**, 053101 (2007); doi: 10.1063/1.2735933

View online: <http://dx.doi.org/10.1063/1.2735933>

View Table of Contents: <http://rsi.aip.org/resource/1/RSINAK/v78/i5>

Published by the [American Institute of Physics](#).

---

### Related Articles

Measurement of an inverse Compton scattering source local spectrum using k-edge filters  
*Appl. Phys. Lett.* **100**, 164104 (2012)

The INE-Beamline for actinide science at ANKA  
*Rev. Sci. Instrum.* **83**, 043105 (2012)

Application of a transmission crystal x-ray spectrometer to moderate-intensity laser driven sources  
*Rev. Sci. Instrum.* **83**, 043104 (2012)

Automated markerless full field hard x-ray microscopic tomography at sub-50nm 3-dimension spatial resolution  
*Appl. Phys. Lett.* **100**, 143107 (2012)

Development of soft x-ray time-resolved photoemission spectroscopy system with a two-dimensional angle-resolved time-of-flight analyzer at SPring-8 BL07LSU  
*Rev. Sci. Instrum.* **83**, 023109 (2012)

---

### Additional information on *Rev. Sci. Instrum.*

Journal Homepage: <http://rsi.aip.org>

Journal Information: [http://rsi.aip.org/about/about\\_the\\_journal](http://rsi.aip.org/about/about_the_journal)

Top downloads: [http://rsi.aip.org/features/most\\_downloaded](http://rsi.aip.org/features/most_downloaded)

Information for Authors: <http://rsi.aip.org/authors>

## ADVERTISEMENT



**HAVE YOU HEARD?**

Employers hiring scientists  
and engineers trust  
**physicstoday JOBS**



<http://careers.physicstoday.org/post.cfm>

# Design and performance of a curved-crystal x-ray emission spectrometer

A. C. Hudson, W. C. Stolte, and D. W. Lindle

*University of Nevada, Las Vegas, Nevada 89154*

R. Guillemin

*Laboratoire de Chimie Physique-Matière et Rayonnement, Université Pierre et Marie Curie-CNRS,*

*11 rue Pierre et Marie Curie, 75231 Paris Cedex 05, France*

(Received 20 December 2006; accepted 2 April 2007; published online 8 May 2007)

A curved-crystal x-ray emission spectrometer has been designed and built to measure 2–5 keV x-ray fluorescence resulting from a core-level excitation of gas phase species. The spectrometer can rotate 180°, allowing detection of emitted x rays with variable polarization angles, and is capable of collecting spectra over a wide energy range (20 eV wide with 0.5 eV resolution at the Cl *K* edge) simultaneously. In addition, the entire experimental chamber can be rotated about the incident-radiation axis by nearly 360° while maintaining vacuum, permitting measurements of angular distributions of emitted x rays. © 2007 American Institute of Physics.

[DOI: [10.1063/1.2735933](https://doi.org/10.1063/1.2735933)]

## I. INTRODUCTION

Molecular photoabsorption is highly anisotropic.<sup>1</sup> Depending on the symmetry of the ground and core-excited electronic states, resonant excitation of inner-shell electrons leads to neutral states with definite orientations of the molecule with respect to the polarization axis of the incoming light. This alignment is preserved through radiative relaxation. Pioneering studies done at the National Bureau of Standards of Washington in the late 1980s showed that x-ray emission from a randomly oriented sample of molecules in gas phase is strongly polarized.<sup>2</sup> Therefore, investigation of atomic or molecular core-level x-ray fluorescence requires intense monochromatic sources of polarized x rays and polarization sensitive high-resolution analytic tool. The first requirement is met by using synchrotron radiation delivered by third-generation light source, which provides inherently linearly polarized x rays.

We describe in this article how the second requirement is met by using a secondary Si(111) crystal spectrometer, which provides good energy resolution and strong rejection of light polarized out of the plane of the crystal surface. Over 99% of light in the plane of incidence is rejected when the crystal angle is near 45° (at 2800 eV).

This spectrometer is of Johann geometry:<sup>3</sup> the crystal and the detector are both situated on a Rowland circle of variable radius with the crystal-to-detector distance fixed. The sample cell is situated inside the circle, rather than on it, to reduce sensitivity to mechanical misalignment of the incoming photon beam with respect to the secondary spectrometer and to prevent point-to-point focusing from the sample to the detector. This geometry increases the angular acceptance of the crystal while maintaining good energy resolution. X rays emitted in a direction perpendicular to the incident radiation from the gas sample are focused onto the detector by a thin variable-radius curved Si(111) crystal. The detector is a position sensitive two-dimensional resistive anode encoder equipped with a stack of three microchannel

plates (MCP-RAE) to amplify the signal and can collect spectra over a wide energy window (20 eV wide with 0.5 eV resolution at the Cl *K* edge) simultaneously. Other similar instruments have been developed: using a curved Si(111) crystal and a one-dimensional position sensitive proportional counter, resulting in a 40 eV wide energy window with a 0.9 eV energy resolution at the Cl *K* edge;<sup>4</sup> using a curved Ge(111) crystal and an interleaved-electrode one-dimensional position sensitive detector, providing a 350 eV energy wide window and a resolution of 5 eV at the Ar *K* edge;<sup>5</sup> using a curved SiO<sub>2</sub> (223) crystal glued on to a machined curved metal block and a two-dimensional charge coupled device (CCD) detector, providing a 130 eV wide energy window and 3–6.7 eV resolution near 8 keV photon energy;<sup>6</sup> and using a multichannel design.<sup>7</sup> The instrument being described in this work is an improvement of an older design.<sup>4</sup> New technical designs of all components produce an instrument that is user friendly with increased resolution.

## II. BEAMLINE 9.3.1

The x-ray spectrometer was specifically designed to be operated at beamline 9.3.1 at the Advanced Light Source (ALS), Berkeley, CA. The technical specifications of this x-ray source have been detailed previously.<sup>8–10</sup> In brief, the ALS provides both quasistatic and pulsed operations. The x-ray emission spectrometer is used preferentially during the quasistatic, or multibunch, mode during which electrons in the storage ring are at an energy of 1.9 GeV with a maximum current of 400 mA. This mode provides intense photon flux essential for molecular x-ray emission measurements. The beamline is equipped with a double Si(111) crystal monochromator to provide

- hard x rays in the 2.2–5.5 keV energy range;
- intense photon flux, 10<sup>11</sup> photons/s; and
- monochromatic light, resolving power  $E/\Delta E = 3000\text{--}8000$  ( $\pm 0.2$  eV at the Cl *K* edge  $\sim 2850$  eV).

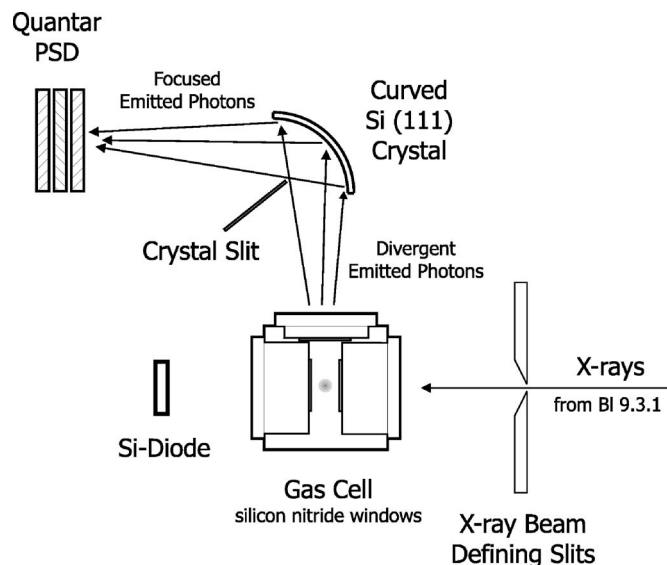


FIG. 1. Schematic representation of the x-ray emission spectrometer experiment. X rays are provided by the Advanced Light Source beamline 9.3.1 which are focused into the gas cell. Resulting x-ray emission is focused onto the position sensitive detector (PSD) by the curved Si(111) crystal.

Focusing of the light is achieved with a matched pair of toroidal mirrors, the first of which collimates the synchrotron radiation from the ALS bending-magnet source, while the second focuses monochromatic x rays onto the target. The beamline is energy calibrated using near-edge x-ray-absorption fine-structure (NEXAFS) scans of well studied chlorinated methanes such as trifluorochloromethane.<sup>11</sup>

### III. SPECTROMETER DESIGN

The spectrometer described here was designed to operate in the 2.4–3.5 keV range, i.e., from the S 1s to the Ar 1s threshold. Light from the beamline monochromator is focused into the chamber housing the emission spectrometer, where a pressure of  $10^{-7}$  Torr is maintained during data collection. Vacuum interlocks are included to protect the beamline and the ALS storage ring should gas containment inside the sample cell fail. The entire experimental chamber can be rotated about the incident-radiation axis by nearly  $360^\circ$  while maintaining vacuum, permitting measurements of angular distributions of emitted x rays. Tilt sensors monitor the chamber rotation (usually  $0^\circ$ – $90^\circ$  relative to horizontal). The incoming photon beam passes through an adjustable four-jaw “slit” to reduce stray and scattered light.

As shown in Fig. 1, the spectrometer itself has three main components: a gas sample cell, a crystal bender, and a position sensitive detector.

Perpendicular to the incoming radiation (and usually positioned vertically upward relative to the gas cell) is a rotary vacuum seal and bellows assembly connecting to the crystal tank, the vacuum housing for the crystal spectrometer. The distance from the gas cell to the crystal face is fixed at 0.4 m. There is an adjustable virtual (Codling-like)<sup>12,13</sup> crystal slit perpendicular to and centered on the crystal face used for alignment purposes and to mask the edges of the crystal in order to improve energy resolution. The entire crystal spec-

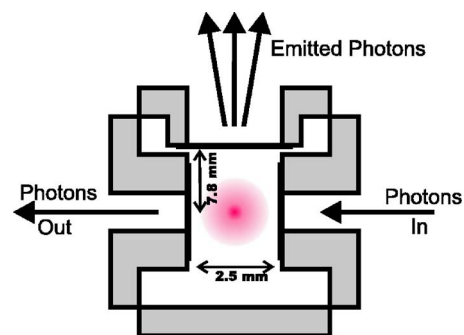


FIG. 2. (Color online) Schematic representation of the gas sample-incident photon interaction region. Incident photons enter and exit the gas cell along the beamline vector, while emitted photons are detected perpendicular to the beamline.

trimeter (with detector) can rotate  $180^\circ$  about the axis defined by the crystal and the sample cell (Fig. 1) and is perpendicular to the incident radiation, due to the rotary seal, allowing detection of emitted x rays with variable polarization angles. Typically, polarization measurements are restricted to two angles, which, in the mostly used vertically oriented geometry, correspond to emitted x rays polarized either parallel ( $0^\circ$ ) or perpendicular ( $90^\circ$ ) to the polarization of the incident radiation. A rotational position transducer determines the angle of polarization being detected, and a second provides a relative angular measurement of the crystal face. Extending from the crystal tank is a 0.6 m long arm leading to the MCP-RAE detector housing. The detector is supported by a curved guide restricting movement of the detector along the Rowland circle. Changing the position of the detector along the guide simultaneously changes the Bragg angle of the spectrometer crystal, changing the energy range of the spectrometer. The relative position of the detector is recorded using a position transducer.

### IV. SAMPLE GAS CELL

A homebuilt static gas cell allows x rays to enter and exit a high-pressure sample of gas while maintaining the high vacuum of the chamber and the beamline. The frame of the gas cell is a commercial minimetall gasket sealed cube, purchased from MDC Vacuum Products Corp. (No. 408000), to which incident-x-ray entrance and emitted-x-ray exit windows and a stainless-steel gas inlet have been added. The entrance and exit windows are  $2\text{ mm} \times 2\text{ mm} \times 200\text{ nm}$  thick silicon nitride ( $\text{Si}_3\text{N}_4$ ) mounted on a  $7.5\text{ mm}^2$  frame. Silicon nitride windows are used because they are easy to obtain, reasonably priced, relatively strong (able to support up to an atmosphere of gas pressure), and have over 90% x-ray transmission in the energy range of primary interest. The entrance and exit windows are mounted on cylindrical tubes extending 9.5 mm into the cube to allow the emission window to observe the entire 2.5 mm photon-beam path through the gas sample (see Fig. 2). Relative absorption measurements can be made using a Si diode to measure the x-ray flux transmitted through the gas cell.

X rays emitted from the gas sample and through the viewing window travel toward the spectrometer crystal. The viewing window is mounted on a cylindrical tube extending

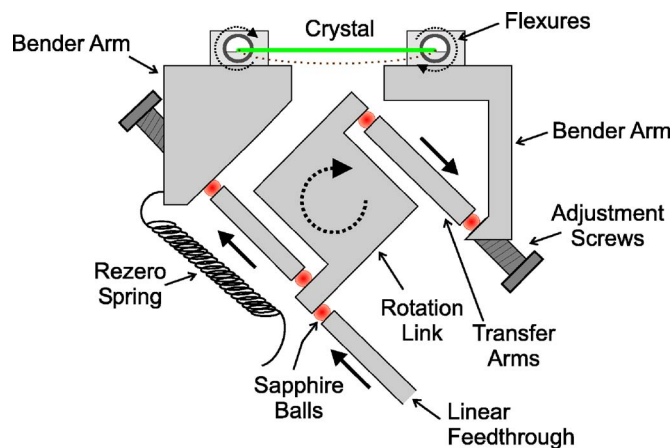


FIG. 3. (Color online) Schematic representation of the crystal bending device. The bend is initiated externally via a linear feedthrough. Extension of the feedthrough pivots the rotation link which causes equal motion on the spreader bars, resulting in identical bending moments at both ends of the crystal.

7.0 mm into the gas cell. The distance the photons travel to exit the sample cell through the viewing window is 7.8 mm. Gas enters the cell through a flange mounted opposite the viewing window, where it remains static during measurements. In order to keep a reasonable ratio between absorption of the incoming x rays and reabsorption of the emitted x rays in the gas sample, we set the sample pressure inside the cell at where the gas absorbs roughly half of the incident photon flux. It corresponds to a pressure of 350 Torr, for instance, for  $\text{CF}_2\text{Cl}_2$ . The sample cell can be pumped or evacuated without disrupting the vacuum inside the chamber. To focus x rays from the beamline into the gas cell, a  $\text{YAlO}_3$  (YAP) crystal and a  $90^\circ$  prism are mounted on the gas cell (outside the viewing plane shown in Fig. 1). The YAP crystal can be moved into the path of the incoming x-ray beam by moving the gas cell which is mounted on an  $x$ ,  $y$ , and  $z$  manipulator. The prism rotates the visible light view of the beamspot created on the YAP crystal, making it possible to monitor the size and shape of the incident-x-ray beam through a vacuum window on the side of the vacuum chamber.

## V. CRYSTAL BENDER

The crystal bender was designed to bend a thin rectangular crystal into a near perfect circular arc, providing focusing and energy tuning of the emitted x rays (see Fig. 3). Radii as small as 0.8 m are produced by the bender, allowing the crystal's radius of curvature to match the diameter of the Rowland circle. This arrangement provides maximum photon focusing in this geometry. In the nominal orientation, the vertical axis of the crystal bender is aligned with the vertical axis of the main chamber, and the entire apparatus is built to be insensitive to gravity for different orientations. The crystal bending device contains two bender arms, a rotation link, two transfer bars, rotary link, pivot flexures for bending, a micrometer controlled linear motion feedthrough, two adjustment screws, a rezeroing spring, and a Si(111) crystal. Bending is initiated when the linear motion feedthrough is moved, thus rotating the rotation link which causes the transfer bars to push the bender arms apart. This action turns the flexures

at both ends of the crystal, producing equal bending moments that deflect the crystal into a circular arc. Flat areas at the ends of the crystal, which do not contribute to the emission spectrum, can be masked with a crystal slit (see Fig. 1). To establish a “zero” for the crystal bender, the crystal is initially set flat and mechanically checked along its length and width for trueness with a micrometer. The crystal can be fine adjusted along its length using the adjustment screws and metal shims. A spring, which attaches the bender arm to the bender housing, forces the crystal back into the flat position after the crystal has been bent. The bender then returns to the flat position when the input bar, attached to the linear motion feedthrough and controlled from the outside of the spectrometer, is completely relaxed. This mounting allows in-vacuum adjustments.

Currently Si(111) crystals are used because they have an effective energy range of 2.0–22 keV. They are also rugged and stable with a high degree of perfection, so they can maintain a curved position for long periods of time without breaking. The size of crystal supported in the bender is 20 mm  $\times$  40 mm  $\times$  0.2 mm thick.

## VI. POSITION SENSITIVE DETECTOR

The position sensitive detector (PSD) is a commercial electron-optical device from Quantar Technology Inc.®, model 3300, and is operated in clean vacuum with pressures lower than  $10^{-6}$  Torr. It has three wafer-type MCP electron multipliers; the first of which has a CsI coating to improve the photon detection efficiency. The MCP stack is backed by a resistive anode position encoder with integrated voltage bias and signal decoupling circuits. Incident photons strike the coated front surface of the first MCP and the electron avalanche diffuses on the uniform resistive sheet surface of the anode toward collection electrodes located at the four corners (A, B, C, and D). The relative charge reaching each of the four corner contacts is a linear function of the position along  $X$  and  $Y$  orthogonal axes of the anode. The four position signals and the signal proportional to the total counts striking the detector, how many x rays are detected, are routed to the detector preamplifiers, an assembly of four preamplifiers (one for each quadrant). All five components are then sent to the position analyzer where the four position signals are converted to  $X$  and  $Y$  coordinates. After the position analyzer, a Quantar Technology model 2401B, the signal passes through a National Instrument PCI-DIO-32HS card (a digital computer card which allows input of the digital  $x$  and  $y$  coordinates signal from the position analyzer), and finally it is displayed, as a 2-D 1024  $\times$  1024 array, and saved using customized LABVIEW software. The images obtained are further processed with the data processing software IGOR from WaveMetrics®, to calibrate and transform the images into emission spectra as a function of energy. As seen in Fig. 4, the raw image from the detector is slightly curved due to the curvature of the crystal. A custom made IGOR fitting procedure accounts for the curvature to obtain maximum energy resolution. A histogram is then created as a function of channel number (0-1023) along the  $X$  axis of the detector. The channel to energy correspondence obtained is typically

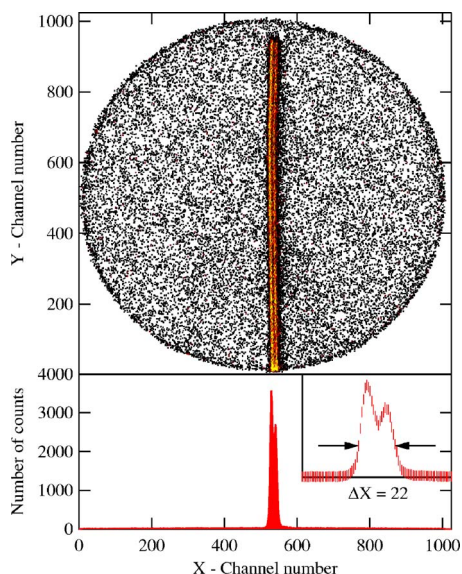


FIG. 4. (Color online) Raw detector image (top) and histogram along the X axis (bottom) after the image was corrected for the curvature with peak widths of 11 channels (1.4 eV). The image recorded in this example is the Cl  $K$  emission from  $\text{CF}_2\text{Cl}_2$  following the  $1a_1, 1b_2 \rightarrow$  continuum excitation (2860 eV photon energy).

$0.122 \pm 0.01$  eV per channel for the  $K\alpha$  emission lines from chlorine ( $\sim 2620$  eV). The detector has a 40 mm active area with a spatial resolution of approximately  $100 \mu\text{m}$ . However, the spectral resolution is not based solely on the spatial resolution of the detector. It includes all experimental effects, namely, natural linewidths, broadening due to diffraction from the crystal, and errors arising from peak-fitting procedures. With this instrument, the combined (beamline and instrumental) measured resolution,  $0.52 \pm 0.05$  eV, is primarily due to diffraction broadening of the crystal, with a very minor part due to the detector spatial resolution. Experimental peak widths in the Cl  $K$ - $L$  energy range vary from 7.2 channels (0.9 eV) on resonance to 11.7 channels (1.5 eV) above resonance and those in the Cl  $K$ - $V$  energy range vary from 13.2 channels (1.4 eV) on resonance to 18.8 channels (2.0 eV) above resonance (Fig. 4). At the Cl  $K$  edge, the natural linewidths are much larger than the experimental resolution and thus determine the majority of the spectral resolution.

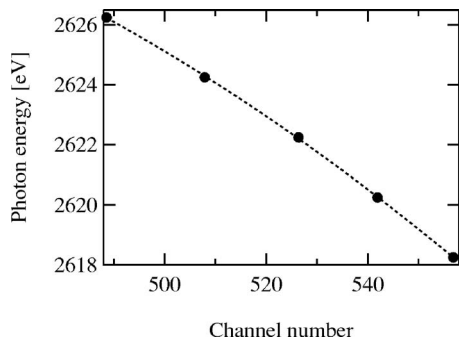


FIG. 5. Energy calibration for the XES spectra. The elastic scattering peak is recorded at five energies to cover the energy window of interest on the detector, and a polynomial fit is calculated through the points.

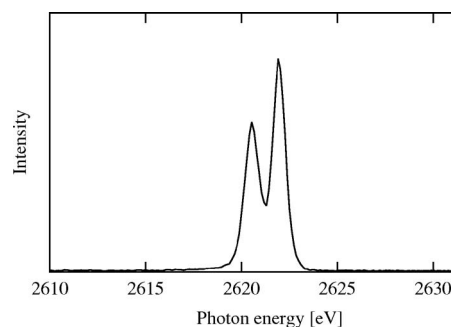


FIG. 6. Cl  $K\alpha$  emission from  $\text{CF}_2\text{Cl}_2$  following the  $1a_1, 1b_2 \rightarrow 13a_1, 9b_2$  excitation (2823 eV photon energy) after energy calibration.

## VII. CALIBRATION

Energy calibration of the x-ray spectrometer is performed in the parallel-polarization direction. Incident photons of the same energy as the emission energy of interest are diffracted off of the sample gas and collected on the detector. Calibration must be done using a parallel orientation because, due to polarization effects, scattered photons are generally not observed in the perpendicular geometry. At least five different incident photon energies are recorded, the range of which covers the window of the measured emission spectra. The energies of the scattered photons are then plotted as a function of peak position determined by the detector (see Fig. 5). A polynomial fit through the points is used to determine the energy of any x-ray emission peaks present within the energy window. As an example, an energy-calibrated spectrum for Cl  $K$ - $L_{2,3}$  ( $K\alpha$ ) emission from  $\text{CF}_2\text{Cl}_2$  following the  $1a_1, 1b_2 \rightarrow 13a_1, 9b_2$  excitation at 2823 eV photon energy is shown in Fig. 6.

In the parallel-polarization geometry, the crystal slit can be used to increase resolution of the x-ray emission spectra, at the cost of reducing both the signal and the width of the energy window. Figure 7 shows the reduction of the usable emission energy window for Cl  $K$ -valence ( $K\beta$ ) emission in the parallel orientation of the spectrometer. The effective

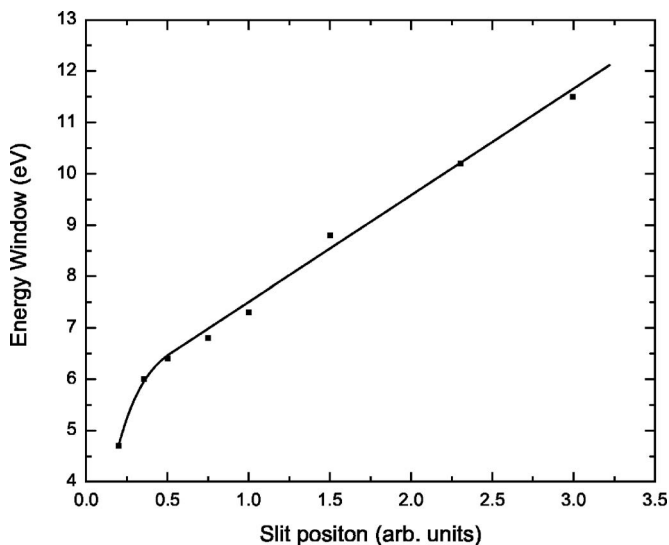


FIG. 7. Variation of the emission energy window with crystal slit position, results taken for Cl  $K\beta$  emission, near 2800 eV.

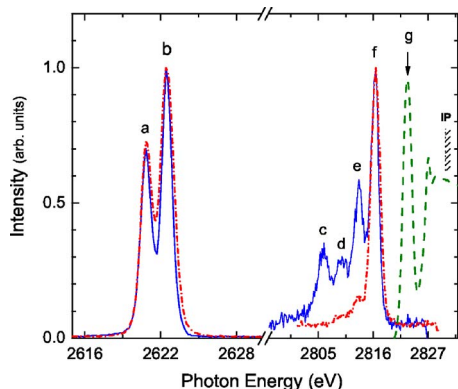


FIG. 8. (Color online) Cl  $K_\alpha$  and  $K_\beta$  emission spectra from  $\text{CF}_2\text{Cl}_2$  following the  $1a_1, 1b_2 \rightarrow 13a_1, 9b_2$  excitation [2823 eV photon energy (g)]. The solid lines represent spectra collected in the parallel orientation, the dotted lines are collected in the perpendicular direction and the dashed line is the Cl  $K$  absorption profile.

resolution follows a nearly linear curve varying from approximately 0.4 eV for a slit of 0.2 to about 1 eV for a slit of 4.0. This relationship between slit position and energy resolution exists because the source volume of x-ray emission is extended along the incident beam axis, which, in the parallel geometry, coincides with the energy-dispersive axis of the spectrometer. In contrast, the resolution and energy window are affected much less in the perpendicular direction, for which the incident beam axis and the energy-dispersive axis do not coincide. For the perpendicular orientation, the only significant consequence is the loss of signal. Similar behavior was observed for Cl  $K-L_{2,3}$  ( $K\alpha$ ) emission.

## VIII. APPLICATIONS

The spectrometer has been used to measure a variety of species, including solids and gases. Figure 8 shows the x-ray emission profile for gas phase  $\text{CF}_2\text{Cl}_2$ , where peaks *a* and *b* are the Cl  $K-L_{2,3}$  fluorescence lines and peaks *c*–*f* are the Cl  $K-V$  lines measured in both orientations. The chlorine  $K$ -edge absorption spectrum is shown as a dashed line. All emission spectra were taken with an incident photon energy on top of the main absorption resonance, *g*, which corresponds to the  $1a_1, 1b_2 \rightarrow 13a_1, 9b_2$  transition at 2823 eV. The solid lines represent measurements taken in the parallel orientation and the dotted lines represent measurements taken the perpendicular orientation. The  $K-L_2$  and  $K-L_3$  lines are present at their characteristic energies [2622.39 (*b*) and 2620.78 eV (*a*), respectively] but do not exhibit the typical 2:1 intensity ratio seen in atomic species, which is due to molecular effects.<sup>14</sup> No polarization effects in the Cl  $K-L_{2,3}$  spectrum are seen at this incidence energy.

In contrast, the  $K$ -valence x-ray emission is highly sensitive to polarization effects below the ionization threshold. In Fig. 8, peak *f* has been scaled to 1 in both spectra for purposes of comparison. A large polarization effect is clearly observed at this incidence energy; peaks *c*, *d*, and *e* essen-

tially disappear in the perpendicular geometry. The observed polarization effect agrees well with previous results.<sup>11,15,16</sup> Polarized x-ray emission was first observed in  $\text{CH}_3\text{Cl}$ .<sup>2</sup> The  $K-V$  emission decay reflects the preferential orientation of the molecules due to the anisotropic nature of x-ray absorption. Polarized x-ray emission can be observed when the rate of radiative decay is much faster than molecular tumbling, as is the case with  $\text{CF}_2\text{Cl}_2$ , and the initial molecular orientation is preserved at the time of relaxation. Such measurements provide crucial information on the symmetry of the molecular orbitals.

## IX. DISCUSSION

Energy resolution improvements of photon and charged particles spectrometers are a major ongoing technical and scientific achievement<sup>4–7</sup> which benefits many different fields in experimental research. Over the last decade, such improvements in x-ray detection has made possible the birth of a new technique called resonant inelastic scattering (RIXS),<sup>17</sup> allowing one to probe x-ray emission with resolutions better than lifetime broadenings, so-called lifetime free spectroscopy. Although based on an older design, the spectrometer presented in this article benefits from new technical developments that have made it possible to improve the energy resolution. It was recently used to probe the femtosecond nuclear dynamics of core-excited gas phase HCl.<sup>18</sup> Such an apparatus combines high resolution and angular capabilities and as such is a unique instrument to perform polarization resolved RIXS measurements.

<sup>1</sup>D. Dill, J. R. Swanson, S. Wallace, and J. L. Dehmer, Phys. Rev. Lett. **45**, 1393 (1980).

<sup>2</sup>D. W. Lindle *et al.*, Phys. Rev. Lett. **60**, 1010 (1988).

<sup>3</sup>H. H. Johann, Z. Phys. **69**, 185 (1931).

<sup>4</sup>S. Brennan, P. L. Cowan, R. D. Henins, D. W. Lindle, and B. A. Karlin, Rev. Sci. Instrum. **60**, 2243 (1989).

<sup>5</sup>B. d'Etat, J. P. Briand, G. Ban, L. de Billy, J. P. Desclaux, and P. Briand, Phys. Rev. A **48**, 1098 (1993).

<sup>6</sup>J. Hozowska, J.-Cl. Dousse, J. Kern, and Ch. Rhême, Nucl. Instrum. Methods Phys. Res. A **376**, 129 (1996).

<sup>7</sup>U. Bergmann and S. P. Cramer, Proc. SPIE **3448**, 198 (1998).

<sup>8</sup>R. C. C. Perera, G. Jones, and D. W. Lindle, Rev. Sci. Instrum. **66**, 1745 (1995).

<sup>9</sup>G. Jones, S. Ryce, D. W. Lindle, B. A. Karlin, J. C. Woicik, and R. C. C. Perera, Rev. Sci. Instrum. **66**, 1748 (1995).

<sup>10</sup>[http://www-als.lbl.gov/als/als\\_users\\_bl/9.3.1-Datasheet.pdf](http://www-als.lbl.gov/als/als_users_bl/9.3.1-Datasheet.pdf)

<sup>11</sup>R. C. C. Perera, P. L. Cowan, D. W. Lindle, R. E. LaVilla, T. Jach, and R. D. Deslattes, Phys. Rev. A **43**, 3609 (1991).

<sup>12</sup>K. Codling and R. P. Madden, J. Appl. Phys. **36**, 380 (1965).

<sup>13</sup>L.-C. Duda, P. Kuiper, D. C. Mancini, C.-J. Englund, and J. Nordgren, Nucl. Instrum. Methods Phys. Res. A **376**, 291 (1996).

<sup>14</sup>A. C. Hudson, W. C. Stolte, R. Guillemin, P. W. Langhoff, J. D. Mills, and D. W. Lindle (to be published).

<sup>15</sup>D. W. Lindle, P. L. Cowan, T. Jach, R. E. LaVilla, R. D. Deslattes, and R. C. C. Perera, Phys. Rev. A **43**, 2353 (1991).

<sup>16</sup>J. D. Mills, J. A. Sheehy, T. A. Ferrett, S. H. Southworth, R. Mayer, D. W. Lindle, and P. W. Langhoff, Phys. Rev. Lett. **79**, 383 (1997).

<sup>17</sup>P. L. Cowan, in *Resonant Anomalous X-Ray Scattering: Theory and Applications*, edited by G. Materlik, C. J. Sparks, and K. Fisher (Elsevier Science, 1994), p. 449.

<sup>18</sup>M. Simon *et al.*, Phys. Rev. A **73**, 020706(R) (2006).